



Erosion behavior of soft, amorphous deuterated carbon films by heat treatment in air and under vacuum

Kazunori Maruyama^a, Wolfgang Jacob^{b,*}, Joachim Roth^b

^a Department of Chemistry, Nagaoka University of Technology, Kamitomioka, Nagaoka 940-21, Japan

^b Max-Planck-Institut für Plasmaphysik, Euratom Association, Boltzmannstrasse 2, D-85748 Garching, Germany

Received 31 March 1998; accepted 15 July 1998

Abstract

The erosion of soft a-C:D films by heat treatment in air and under vacuum is studied by ion-beam analysis. When the films are heated in air above 500 K, the film thickness and the areal densities of C and especially D decrease, and oxygen is incorporated in the films. The initial atomic loss rates of carbon and deuterium from the films are 2.6×10^{17} C atoms $\text{cm}^{-2} \text{h}^{-1}$ and 4.8×10^{17} D atoms $\text{cm}^{-2} \text{h}^{-1}$ at 550 K. However, after D depletion the films show a resistivity against further erosion due to annealing in air. When the films are heated under vacuum erosion starts at about 600 K and all components including D decrease proportionally to the film thickness. Thermal desorption spectroscopy of the films reveals the evolution of C_xD_y type hydrocarbons. Infrared analysis shows that the incorporated oxygen is chemically bonded to carbon. The thermally-activated decomposition of the soft a-C:D films is compared to that of hard a-C:D films and a reaction scheme is suggested. © 1999 Elsevier Science B.V. All rights reserved.

1. Introduction

There is no material which shows so many different forms and structures as carbon, ranging from graphite, fullerenes and diamond for the pure materials to polymeric materials such as polyethylene for compounds with hydrogen. Amorphous hydrogenated carbon (a-C:H) films are a further example of interesting carbon-containing materials. Hard a-C:H films are often named diamond-like carbon (DLC) because of their chemical inertness, hardness, electrical insulating properties and predominant sp^3 hybridization as in diamond [1]. Such hydrogenated carbon films are usually produced from low-pressure glow discharges in hydrocarbon gases. The properties of these films may vary over wide ranges depending on the specific deposition conditions [1–4]. Hard a-C:H films are deposited if energetic ions with energies above about 50 eV participate in the deposition process. At low-energy ion bombardment polymer-like, soft films are produced. Hard and soft films are easily

distinguished by their mechanical properties. Hard films are very scratch resistant while soft films can easily be scratched with a metallic pin. But the films show significant differences in almost all of their physical properties. For example, hard a-C:H has typically an H/C ratio of 0.4, a density around about $1.5\text{--}2 \text{ g cm}^{-3}$, and a refractive index, n , of 2 and higher. Soft films, on the other hand, possess an H/C ratio of 1 and higher, densities down to 1 g cm^{-3} , and n around 1.5 [1–4]. However, the transition between soft and hard films is gradual and prevents a clear distinction.

As protection material of the first wall of tokamak plasma experiments, hard a-C:H films were deposited in situ by plasma chemical vapor deposition using dc, rf and electron cyclotron resonance (ECR) discharges such that metal impurities in tokamak plasmas were significantly reduced [5]. However, films deposited during fusion plasma discharges onto limiters and protective tiles are often porous, soft a-C:D films. The hydrogen inventory in these redeposited films is a considerable concern in fusion experiments using D/T mixtures. It presents a potential environmental risk during vacuum vessel maintenance and possible accidental vacuum loss. Therefore, the interaction of redeposited films with air

* Corresponding author. Tel.: +49-89 3299 2618; fax: +49-89 3299 1149; e-mail: jacob@ipp.mpg.de

and different atmospheric gases was investigated in the past [6–9]. Furthermore, removal of redeposited films by oxidation at elevated wall temperatures has been proposed as *in situ* cleaning method [10–12]. With respect to erosion of redeposited films, it is important to know the quantitative removal rates of carbon and hydrogen isotopes from a-C:H films. From the viewpoint of tritium inventory in such films, it is of interest to investigate the reduction of the tritium inventory by isotope exchange with deuterium and hydrogen. For this purpose, deuterated carbon films are a suitable system for investigation because it is possible to distinguish the lost deuterium from hydrogen incorporated in the film from the residual gas. Wang et al. reported the erosion of hard a-C:D films by heat treatment and showed that the surface deuterium is quantitatively balanced by oxygen uptake and hydrogen isotope exchanges in the film until deuterium is completely released [12]. This paper describes similar studies of the erosion behavior by annealing of soft a-C:D films with a large initial hydrogen content in vacuum and air and of changes in the films stoichiometry and structure during annealing.

2. Experimental

Amorphous deuterated carbon (a-C:D) thin films were prepared by capacitively coupled 13.56 MHz radio-frequency plasma deposition using research grade precursor gases (CD_4 , D_2 ; 99% purity). A detailed description of the deposition apparatus is given elsewhere [13]. As substrate material we used p-type single crystalline silicon. Substrates about $1 \times 1 \text{ cm}^2$ in size were cleaned in an ultrasonic bath with acetone, isopropanol and distilled water directly before they were inserted in the deposition chamber. After a base pressure of 5×10^{-5} mbar was reached (usually after pumping over night), the substrates were etched in a hydrogen plasma (4 Pa, -300 V dc self-bias) for 1 h in order to reduce the surface oxide layer.

Two sets of samples, each consisting of about 20 samples, were deposited for the experiments described in this paper. Soft a-C:D films (set A) were deposited under the following conditions: CD_4 flow rate $30 \text{ cm}^3 \text{ STP}$, pressure 8 Pa, applied RF power density of 0.15 W cm^{-2} (averaged over the surface of the substrate electrode 10 cm in diameter) resulting in a dc self-bias of -60 V , and substrate temperature 300 K. Soft a-C:D:H films (set B) were deposited from a mixed gas flow of CD_4 and H_2 ($30 \text{ cm}^3 \text{ STP}$ each) at a pressure of 6 Pa applying a dc self-bias of -40 V (RF power density of 0.10 W cm^{-2}). The deposited film thickness was monitored *in situ* by means of a He–Ne laser interferometer.

The heat treatment of the films in air was carried out using a furnace at ambient atmosphere applying temperatures up to 800 K [12]. Annealing in vacuum was

performed in two different UHV chambers. In the first chamber with a base pressure of 2×10^{-10} mbar the samples were mounted on a stainless steel substrate holder which was radiatively heated by a tungsten wire. The temperature was measured by a thermocouple immersed in a bore of the substrate holder. The surface temperature in this device was checked previously with pyrometry. Good agreement between the temperatures measured by the thermocouple and the optical pyrometer was found. The second chamber, dedicated to thermal desorption spectroscopy (TDS) [14], had a base pressure of 1×10^{-9} mbar. In this device the samples were heated by passing a dc current through the silicon substrate. A heating rate of 15 K min^{-1} was applied controlled by the signal from a thermocouple pressed to the back of the substrate. The temperature was calibrated by optical pyrometry at temperatures above 750 K, thus correcting the thermocouple reading which was lower than the true substrate temperature due to imperfections of the thermal contact between thermocouple and substrate. Due to this recalibration of the sample temperature the true heating rate was 16.7 K min^{-1} . The uncertainty of the so determined temperature was estimated to be about $\pm 20 \text{ K}$. For all annealing experiments we used a fresh sample for each individual annealing temperature.

For the measurement of thermal desorption spectra, the evolved gases were examined with a quadrupole mass analyzer in line-of-sight with the substrate surface. The set up allowed to record either 16 different masses as a function of time or a complete mass spectrum one after another. Usually TDS spectra were recorded using the first mode, but in some experiments we measured mass spectra ranging from 1 to 200 amu to investigate the total composition of the evolving gas flux. In these experiments mass spectra were recorded consecutively with a scan time of about 40 s for a complete run. Under the chosen experimental conditions, this corresponds to a difference of about 12 K between consecutive mass spectra. Before a TDS measurement the samples were heated to 380 K in the apparatus over night at a pressure below 10^{-7} Pa in order to reduce background signals from water vapor, carbon monoxide and carbon dioxide in the system. Due to this preannealing, no information can be anticipated for temperatures lower than about 400 K for the TDS measurements presented here. In experiments without this preannealing step no additional desorption peaks were detected in the range up to 400 K, and the TDS spectra showed no principal difference beside a significantly higher background of H_2O , CO and CO_2 .

The stoichiometry of the films was analyzed using ion-beam analysis (IBA). The absolute concentrations of H and D were determined by elastic recoil detection (ERD) at a scattering angle of 30° using a beam of He^+ ions ($E = 2.6 \text{ MeV}$) from a van de Graaff accelerator.

The absolute concentrations of C and O were determined by elastic scattering of protons with enhanced cross section (PES) using a beam of H^+ ions ($E=1.5$ MeV) with a scattering angle of 165° . The reaction cross-sections used for the determination of the components were taken from Refs. [15–17]. Infrared spectra were measured using a Perkin–Elmer Fourier-transform infrared spectrometer (1760X).

After deposition, the film thickness d_s was determined mechanically with a Tencor Alpha Step 200 profilometer after partial removal of the film by scratching without scratching the silicon substrates. This is easily possible for the soft films used in this study. The accuracy of a single thickness measurement is about 5 nm. An additional uncertainty in the thickness measurement arises from a slight inhomogeneity of the layers, which is in general below 10%. To exclude this uncertainty from the measurements of the thickness change of the same film before and after heat treatment, it was assured that the thickness was measured at the identical position on the sample. In general, thickness measurements were performed at several positions on one sample to reduce statistical errors. The mass densities and atom number densities were calculated from the areal densities measured by ion-beam analysis and the mechanically determined thickness d_s . With the measured film thickness d_s the refractive index n was calculated according to $n = \lambda_{\text{HeNe}} m / 2d_s$, with m being the number of interference cycles of the He–Ne laser interferometry signal and λ_{HeNe} the wavelength of the He–Ne laser (632.8 nm).

3. Results

3.1. Characterization of soft a-C:D films

Table 1 shows the elemental densities of a-C:D and a-C:D:H films (sets A and B) before heat treatment determined by PES and ERD analyses together with the thicknesses and refractive indices of the films. The films used in this study are about 300 nm thick and possess properties typical of soft, polymer-like a-C:D layers. The refractive indices are low, between 1.55 and 1.58. The atom densities of carbon are also low, between 4.4 and $4.5 \times 10^{22} \text{ cm}^{-3}$, compared to the density of about $8 \times 10^{22} \text{ cm}^{-3}$ of carbon in hard a-C:D films [12]. The

atomic ratio of D/C is around 1 being significantly higher than the value of about 0.4 for hard a-C:D films [1,12]. Due to the difference in the deposition conditions, the two sets of samples differ in their specific properties. The most obvious contrast is the difference in the (D+H)/C ratio. The soft a-C:D films (set A) have a ratio of 0.96 while the soft a-C:D:H films (set B) have 1.34. The carbon atom density is quite similar for both films while the total atom density for set B is about 10% higher than for set A. This is due to the significantly higher hydrogen isotope content of set B. The hardness of the films was not explicitly measured, it was only determined by a very crude, qualitative scratch test using a small screw driver. In fact, the films investigated in this study could be easily scratched by a metal driver while it was impossible to scratch the hard films investigated in the preceding study [12]. The films of set A were deposited from 99% pure CD_4 , but oxygen and hydrogen were found in the films by ion-beam analysis (below 10% each, see Table 1), and C–O and C–H functional groups were detected by infrared analysis. We assume that oxygen and hydrogen were incorporated through the reaction of the films with oxygen and water vapor after they were exposed to air. This behavior has also been found for other soft, polymer-like films [14]. This is a strong indication that soft a-C:H or a-C:D films are chemically not completely stable in air, but they incorporate oxygen and hydrogen from the environment.

3.2. Heat treatment of soft a-C:D and a-C:D:H films in air

Samples from both deposition runs (sets A and B) were exposed to an identical heat treatment. These samples were heated in air at different temperatures for 1 h each. Fig. 1 shows film thickness and the areal densities of C, O, H and D as a function of the annealing temperature. Since the thicknesses of the original films before annealing were slightly different from each other, ranging from 290 to 315 nm for set A and from 280 to 320 nm for set B, the areal densities plotted in Fig. 1 are renormalized to 300 nm as the initial thickness before annealing to allow a quantitative comparison. The individual thickness of each film was measured before and after annealing and the relative thickness change was calculated.

Table 1
Physical properties of the investigated films

	Sample	dc self-bias voltage (V)	Thickness (nm)	Refractive index	Composition (10^{22} cm^{-3})				(D+H)/C
					C	O	D	H	
Set A	Soft a-C:D	–60	305	1.55	4.5	0.7	3.9	0.4	0.96
Set B	Soft a-C:D:H	–40	300	1.58	4.4	0.3	4.4	1.4	1.34
Ref. [12]	Hard a-C:D	–350	730		9.0	–	3.9	–	0.43

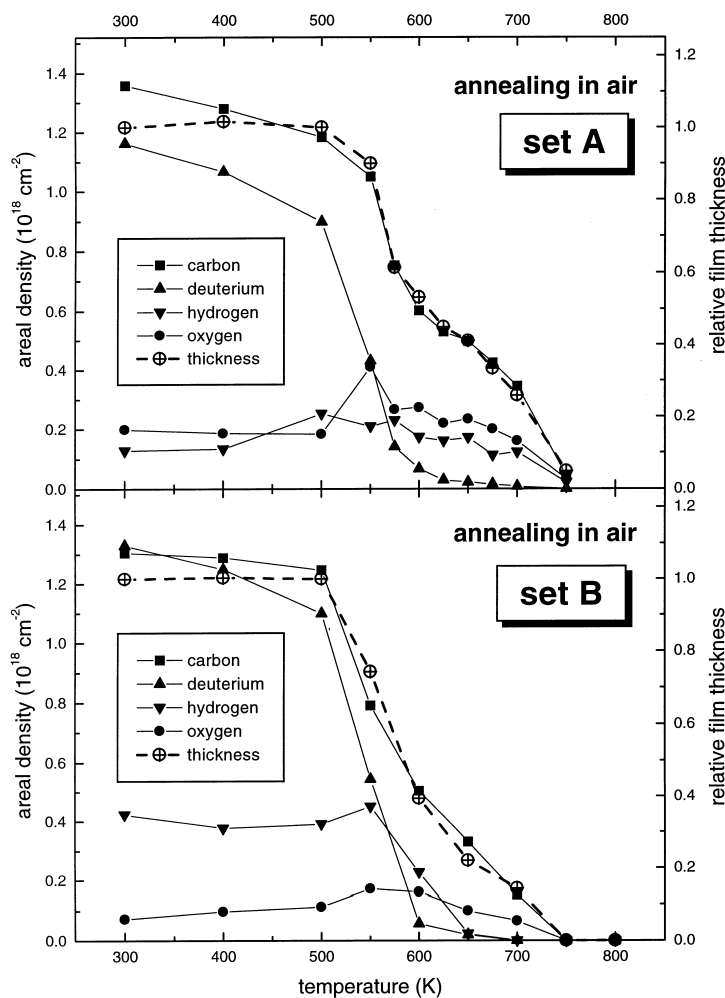


Fig. 1. Film thickness and areal densities of C, O, H and D of soft a-C:D (set A, top) and a-C:D:H (set B, bottom) films heated in air for 1 h as a function of annealing temperature. For each annealing step a fresh sample was used. The initial film thickness was between 290 and 315 nm for the films from set A and between 280 and 320 nm for set B. The areal densities are renormalized to a thickness of 300 nm to allow direct comparison.

We can see in Fig. 1 that the a-C:D film thickness does not decrease if heated to temperatures below 500 K while the amounts of both carbon and deuterium decline by about 10% indicating a reduction of the carbon and deuterium density. At temperatures higher than 500 K for both sets of samples the decrease of the carbon areal density correlates very well with the decrease of the film thickness while deuterium is lost rapidly between 500 and 600 K. Since the decomposition of the films in air proceeds slightly different from each other, we first discuss the results for set A. The loss of deuterium is accompanied by a steep increase of the amount of oxygen and a loss of carbon. After almost all deuterium is released around 600 K, carbon declined to about one-half of its initial value and the further decrease in film thickness is not as rapid as for temperatures below 600

K. At temperatures above 675 K the erosion accelerates again. The loss of carbon for set B shown in the lower part of Fig. 1 is faster than for set A and the plateau in the range between 600 and 700 K does not occur or lies at least much lower. Similar to set A the loss of deuterium is accompanied by an increase of the amount of oxygen, although this increase is smaller than for set A.

Fig. 2 shows a sequence of compositional profiles after different annealing temperatures for samples from set A. The virgin sample contains about equal amounts of carbon and deuterium and the oxygen and hydrogen incorporated from the ambient atmosphere after deposition are distributed homogeneously throughout the whole film thickness. Obviously, the layer is permeable for these gases. The reason for this could be the low mass density (1.2 g cm^{-3}) leading also to a low atom

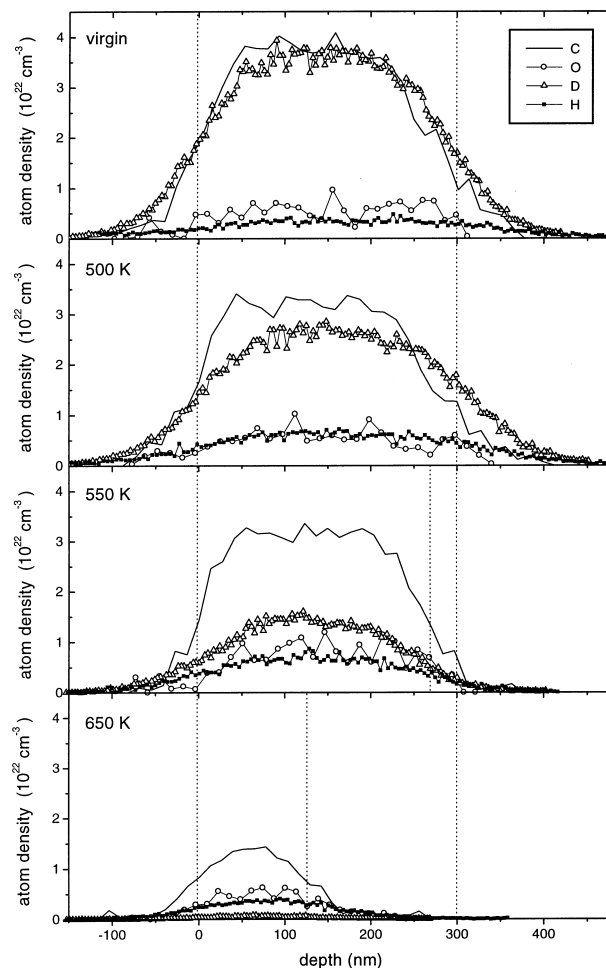


Fig. 2. Depth profiles of the atomic concentrations determined by ion-beam analysis after the thermal treatment of some films from set A shown in Fig. 1. The annealing temperature is indicated in the figure. The initial film thickness of 300 nm and the thickness of the remaining film as measured by profilometry is indicated by the dotted lines.

density of $9.5 \times 10^{22} \text{ cm}^{-3}$ of the material. This is roughly 20% lower than the atom density of graphite ($11.3 \times 10^{22} \text{ cm}^{-3}$), but due to the substantial hydrogen content the carbon atom density is only $4.5 \times 10^{22} \text{ cm}^{-3}$ (see Table. 1) being less than 50% of the graphite value. The figure demonstrates that the loss of deuterium is accompanied by an oxidation of the remaining material. Annealing in air for 1 h at 500 K does not cause a substantial loss of carbon, but the amount of deuterium decreases slightly while oxygen and hydrogen increase. The total atom density decreases to about $8.4 \times 10^{22} \text{ cm}^{-3}$. At 550 K the deuterium concentration drops significantly and the decrease of the film thickness starts. The atom density reduces to $7.8 \times 10^{22} \text{ cm}^{-3}$. At 650 K the remaining film thickness is 125 nm. At film thicknesses below 150 nm the depth resolutions of the ion-beam analysis is insufficient to resolve the profiles. As the resolution is different for ERD and PES analysis the

elemental concentrations do not add up to 100% at these thicknesses in Fig. 2. This causes the apparent drastic drop of the atom density in the remaining film. However, the real atom density determined from the film thickness and the integral areal densities remains around $7.6 \times 10^{22} \text{ cm}^{-3}$. Still, this is a rather low value and the remaining material has a low mass density of 1.34 g cm^{-3} . As a consequence, the remaining material has to be considered as a rather porous structure.

In contrast to hard films [12] where the oxidation started at the surface, the compositional changes for the soft films occur at all depths throughout the whole film. This indicates that the soft, polymer-like films are permeable for reactive gases from the ambient atmosphere, while hard films are not permeable. With the onset of the thickness loss the relative composition of the film changes substantially. The fractions of oxygen and hydrogen in the films increase from initially 7% and 5% to

about 22% and 18%, respectively. This fraction is rather independent of the annealing temperature for temperatures above about 600 K. This effect is not so obvious in Fig. 1, which shows the integral data, because the film thickness decreases with increasing annealing temperature, but it becomes visible in the depth distributions of Fig. 2.

Fig. 3 presents the results for annealing in air at constant temperatures of 550 and 650 K, respectively, as a function of annealing duration. At 550 K (Fig. 3(a)) the thickness decreases monotonously with the annealing duration. In the first hour we find again a decrease of the density. The thickness decreases by about 10% and the carbon areal density by 15%. For longer annealing durations the thickness is again in excellent agreement

with the amount of carbon. The rate of change decreases with prolonged annealing duration and almost steady state is reached after 8 h of annealing. After 8 h the thickness drops to 45% and the carbon content to 42% of the virgin sample. The loss of deuterium from the film proceeds much faster than the carbon and thickness decrease. After 2 h more than 80% of the initial deuterium is released and after 8 h only 5% is left. The total amount of hydrogen increases in the first 2 h and then remains rather constant. The total amount of oxygen increases in the first hour, then declines proportional to the thickness. For annealing durations longer than 2 h the composition of the remaining material is rather constant, only the thickness and the total amount decline slowly. The average composition after 2 h at 550 K

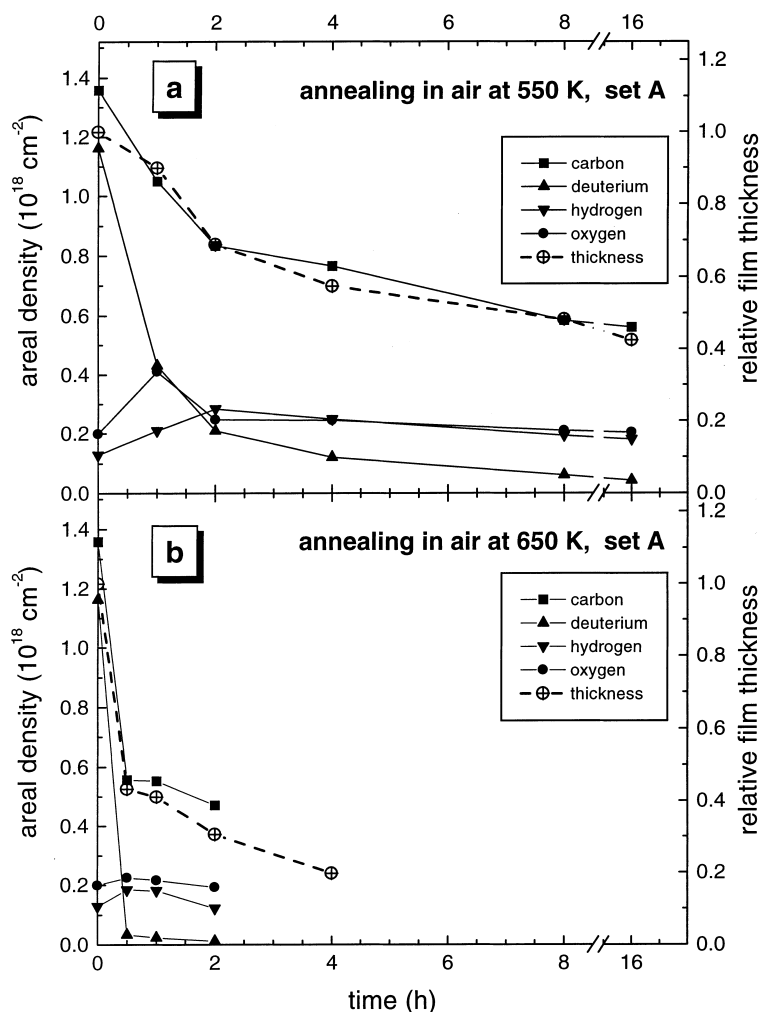


Fig. 3. Film thickness and areal densities of C, O, H and D of soft a-C:D films (set A) heated in air at a constant temperature of 550 K (a) and 650 K (b) as a function of annealing duration. For each annealing step a fresh sample was used. The initial film thickness was between 280 and 320 nm. The areal densities are renormalized to a thickness of 300 nm to allow direct comparison. Please observe the x axis break.

is C:O:(D+H) = 0.53:0.20:0.27. The initial loss rates for carbon and deuterium averaged over the first two hours are 2.6×10^{17} C atoms $\text{cm}^{-2} \text{h}^{-1}$ and 4.8×10^{17} D atoms $\text{cm}^{-2} \text{h}^{-1}$.

At a temperature of 650 K, shown in Fig. 3(b), the general behavior is quite similar, but decomposition proceeds on a much faster time scale. After 0.5 h the thickness drops to 40% and almost all deuterium is gone. For longer durations the thickness decreases slowly and the composition stays rather constant at about C:O:(D+H) = 0.56:0.23:0.21. The initial loss rates for carbon and deuterium at 650 K in the first 30 min are 1.6×10^{18} C atoms $\text{cm}^{-2} \text{h}^{-1}$ and 2.3×10^{18} D atoms $\text{cm}^{-2} \text{h}^{-1}$. This is roughly a factor of 5 higher than at 550 K.

3.3. Infrared analysis

The infrared spectra of the films before and after annealing at 550 K are shown in Fig. 4. They are presented as a function of the extinction coefficient, κ (the imaginary part of the complex refractive index) vs. the wave number. These spectra were calculated applying a formalism which was recently described [18]. It allows one to calculate the complex refractive index from measured thin film infrared spectra taking into account multiple coherent reflections in the films themselves, multiple incoherent reflection in the substrate and the Kramers–Kronig-relation between the real and imaginary part of the refractive index.

In the infrared spectrum of the film before annealing (bottom line in Fig. 4) we recognize three clearly visible absorption bands partly superimposed on a broad, slowly varying feature. The bands are located at around 2100–2250, 1720 and 1060 cm^{-1} . Küppers et al. reported infrared spectra of a-C:H and a-C:D films and they assigned the band around 2100–2250 cm^{-1} to the various sp^2 and sp^3 C–D stretching vibrations [19,20]. The absorption peak at 1720 cm^{-1} is an absorption typical of the C=O carbonyl group [21]. We assign the absorption at 1060 cm^{-1} to Si–O stretching vibrations because, on the one hand, it does not change much with annealing duration and, on the other hand, it is also visible as a strong absorption peak on a silicon substrate without carbon film heated in air at 800 K. Fig. 4 indicates that the C–D absorption band around at 2200 cm^{-1} is almost completely lost after annealing for 2 h. With increasing annealing duration the carbonyl band at 1720 cm^{-1} increases in intensity and new absorption bands appear at 1780, 1610, 1430 and 1225 cm^{-1} . We assign these bands to the C=C stretching vibration (1610 cm^{-1}) and to the –COO– (ester group) at 1780 cm^{-1} (C=O) and 1225 cm^{-1} (C–O). The band at 1430 cm^{-1} is tentatively assigned to the in-plane deformation band of the –C–O–H group. C–H or C–D bending vibrations cannot account for the increased intensity in this wave number range because the corresponding stretching vibrations at around 3000 and 2200 cm^{-1} , respectively, are either completely absent or decline with increasing annealing duration.

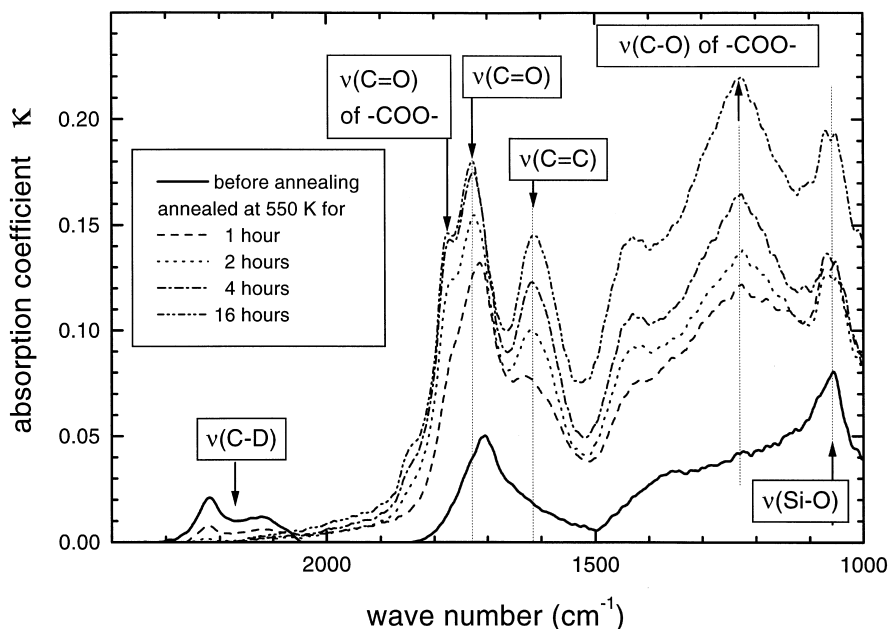


Fig. 4. Infrared spectra (κ spectra, see text) of soft a-C:D films (set A) annealed in air at 550 K for various durations (identical samples as used in Fig. 3).

The new bands become stronger with increased annealing duration. We interpret this behavior as an increase of the density of the respective groups in the remaining film. This is in perfect agreement with the quantitative ion-beam analysis results from Fig. 3 which show, on the one hand, a very rapid decrease of the deuterium content within the first 2 h of annealing and, on the other, an increase of the oxygen concentration. The rapid decrease of the deuterium leads to the formation of C=C double bonds and consequently to an increase of the band at 1610 cm^{-1} . Another possible explanation for the increase of the 1610 cm^{-1} band is, however, that the transition dipole moment of this band increases due to neighboring polar $\text{C}=\text{O}$ and COO -groups. It should be noted that in addition to the bands shown in Fig. 4 we also detect a significant increase of OH bands at around 3250 and 3500 cm^{-1} . Infrared analysis of the films exposed to air at 650 K (Fig. 3(b)) yields results very similar to those shown in Fig. 4. On the other hand, films annealed in vacuum (see Section 3.4, Fig. 5) did not show an increase of the bands in the range between 1100 and 1750 cm^{-1} . Only the C–H and C–D related bands decreased more or less proportional to the hydrogen and deuterium content, respectively.

Infrared analysis clearly indicates that oxygen is chemically incorporated in the films and a large fraction of it is bonded in carbonyl and ester groups. Since we find no increase of the C–H stretching vibrations around 3000 cm^{-1} we assume that the incorporated hydrogen, which is seen by ion-beam analysis, is bonded in the form of OH groups which are also detected by infrared analysis. This is a strong indication that no effective

thermally-activated hydrogen isotope exchange occurs during annealing in air.

3.4. Heat treatment of soft a-C:D:H films in vacuum

Soft a-C:D:H films prepared at a dc self-bias of -40 V bias from the mixture of CD_4 and H_2 (set B) were used to study the thermal decomposition under vacuum. The results are presented in Fig. 5. The behavior is different from that of annealing in air shown in Fig. 1 for identical films. No significant changes occur up to about 550 K besides a small loss of carbon and deuterium. For higher temperatures the loss of carbon is accompanied by a proportional loss of both hydrogen isotopes and a decrease in thickness, but in contrast to annealing in air no additional oxygen is incorporated. Decomposition of the films occurs at temperatures about 50 K higher than in air. Quite remarkable is the fact that for this sample almost all carbon disappears in volatile products although no reactive atmosphere is present. This means, in other words, that these soft films sublime completely in vacuum.

The distribution of released products was investigated by thermal desorption spectroscopy (TDS). Fig. 6 shows TDS spectra of an a-C:D (set A) film. In this figure the quadrupole mass analyzer (QMS) signals for the mass numbers (m/e) 4, 20, 28, 32, 44 and 46 amu are plotted as a function of the substrate temperature. The signals shown are raw data from the mass spectrometer. They are neither corrected for the mass-dependent transmission of the quadrupole and the species-dependent sensitivity factors, nor is any background subtracted. This means that these data cannot be interpreted

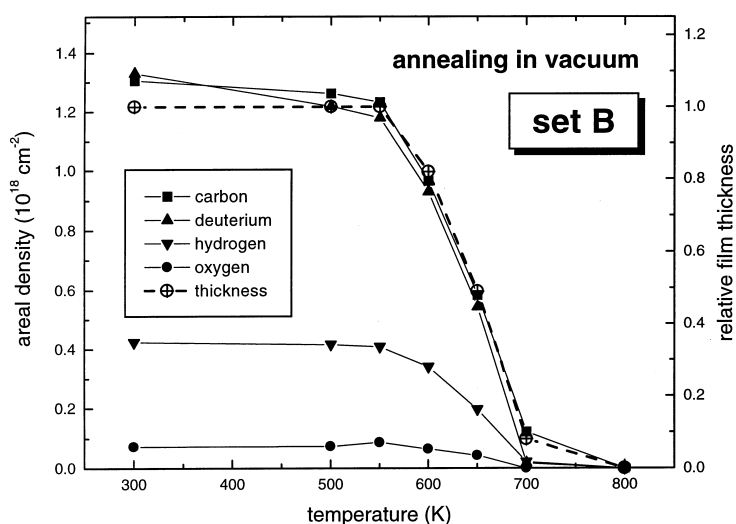


Fig. 5. Film thickness and areal densities of C, O, H and D of soft a-C:D:H films (set B) annealed in vacuum for 1 h as a function of annealing temperature. For each annealing step a fresh sample was used. The areal densities are renormalized to a thickness of 300 nm to allow direct comparison.

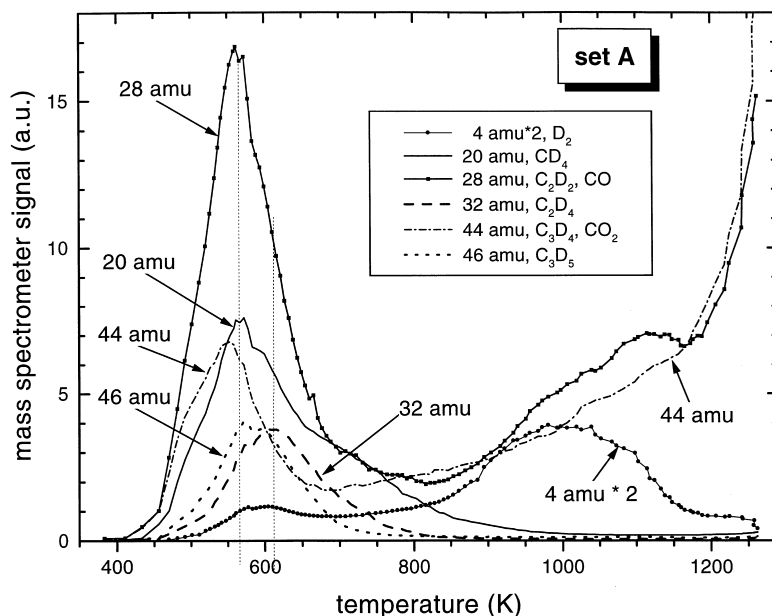


Fig. 6. Thermal desorption spectra of a soft a-C:D film (set A) monitored at mass numbers of 4, 20, 28, 32, 44 and 46. The vertical lines correspond to the temperatures of the mass spectra shown in Fig. 7.

quantitatively, but they allow to get a qualitative impression of the released products. The signals 28 and 44 amu at temperatures above about 800 K are assigned to CO and CO₂, respectively, as these mass numbers are usually detected as strong background signals. The water peak at 18 amu shows an identical increase for temperatures above 800 K. Background signals of these mass numbers measured using a plain silicon substrate show the same exponential rise at temperatures above 900 K. However, no large peaks in the temperature range from 300 to 800 K such as these depicted in Fig. 6 were found in these background measurements. Therefore, the maxima in Fig. 6 for 28 and 44 amu around 500 K are assigned to the evolved gases from the a-C:D film. The most probable candidates for these mass numbers are C₂D₂ and CO at 28 amu and C₃D₄ and CO₂ at 44 amu. A clear distinction between these gases cannot be made on the basis of the presently available data, but they originate unambiguously from the film and not from the background. Because the virgin films contain about 10% oxygen (cf. Fig. 1 and Table 1), formation of CO and CO₂ in the film is conceivable so that these gases contribute to the respective mass peaks. However, since the total oxygen content in the layers is not very high, we assume that CO and CO₂ do not dominate the mass peaks at 28 and 44 amu and assign them predominantly to C₂D₂ and C₃D₄, respectively. This assignment is supported by the presence of peaks at mass 20 (CD₄), 32 (C₂D₄), and 46 (C₃D₅) (cf. Fig. 6), and other deuterated hydrocarbon fragments not shown in Fig. 6 showing all the identical temperature dependence.

The dominant peak in the spectrum is at $m/e=28$ amu. Gas evolution at 28 amu starts around 450 K, increases to a maximum at around 560 K and gradually decreases up to 800 K. It is presently unclear whether the two small peaks at 1000 and 1100 K are background emission of CO or whether they originate from the layer. The onset of gas evolution at 44 amu is also at 450 K, but it rises faster than that at $m/e=28$ and declines more quickly. The peak shape for 20 amu is very similar to 28 amu, but we find a shoulder at higher temperatures (700 K). The evolution of C₂D₄ (32 amu) and C₂D₅ (46 amu) also begins at around 450 K, but the maxima are shifted to about 610 and 590 K, respectively. Further spectra, not shown in Fig. 6, were recorded at 30 (C₂D₃), 48 (C₃D₆), and 60 amu (C₄D₆). The peak shape of these three peaks is identical to that of the 46 amu spectrum while the intensities relative to the 46 amu spectrum are 1, 0.25 and 0.07, respectively. The presence of these peaks strongly supports the assignment of all these peaks to deuterated C_xD_y molecules. In contrast to the deuterium release in form of hydrocarbons, the evolution of D₂ (4 amu) begins at temperatures higher than 850 K and increases to reach a maximum at around 1000 K. The intensity at 4 amu in the range from 400 to 850 K is probably due to the cracking of larger C_xD_y molecules. This implies that the deuterium loss of soft a-C:D proceeds in vacuum via the release of volatile deuterated hydrocarbon molecules in the initial stage (400–850 K) and via D₂ at temperatures above 850 K. The latter temperature is in good agreement with the release of hydrogen from hard a-C:H films [14,20,22].

Fig. 7 shows two mass spectra in the range from 1 to 100 amu recorded during annealing in the TDS chamber. Fig. 7(a) is recorded at a temperature corresponding to the maximum of the mass 28 peak (560 K) and Fig. 7(b) corresponds to a temperature slightly higher than the maximum of the mass 32 peak (620 K). Please observe that the y axis in Fig. 7(a) is broken because the mass 28 peak is so strong in this spectrum. Besides this very pronounced intensity difference of the 28 amu peak, the spectra are rather similar. We can clearly distinguish the groups corresponding to C_1D_y molecules (18 and 20 amu), C_2D_y (28, 30, and 32 amu), C_3D_y (42–50 amu), and higher hydrocarbons. It is quite remarkable that fragments up to mass 98 corresponding to C_7D_7 are detectable. The alternating intensities of the mass peaks with the even mass number being always stronger than the odd ones strongly supports the assignment of all these peaks to C_xD_y molecules. The odd numbered peaks may be due to mixed hydrogen isotope molecules from the film, since the film contained a few percent hydrogen, or they may be formed in isotope exchange reactions at the chamber walls or in the ionizer of the mass spectrometer.

4. Discussion

The decomposition of soft a-C:D films depends critically on the film structure and differs significantly from that of hard a-C:D films [12]. In this context it has to be kept in mind that a smooth transition between the properties of soft and hard a-C:D films prevents a clear distinction. A reasonable first indicator of the film properties and of the thermal stability and instability, respectively, is the initial hydrogen isotope content or the (D+H)/C ratio of the film. It was shown in Figs. 1, 3 and 5 that the film structure slightly changes at temperatures in the range up to 500 K. This happens during annealing in air as well as in vacuum and is documented in the decrease of the film density. We attribute this effect to a release of intrinsic mechanical stress originating from the deposition process. A similar reduction in density during annealing was also observed for the hard a-C:D layers in the preceding study [12] and for other soft and hard a-C:H films [14] and seems to be a quite general feature. For temperatures above 500 K the thickness decreases proportional to the decrease of the carbon areal density indicating no notable changes in

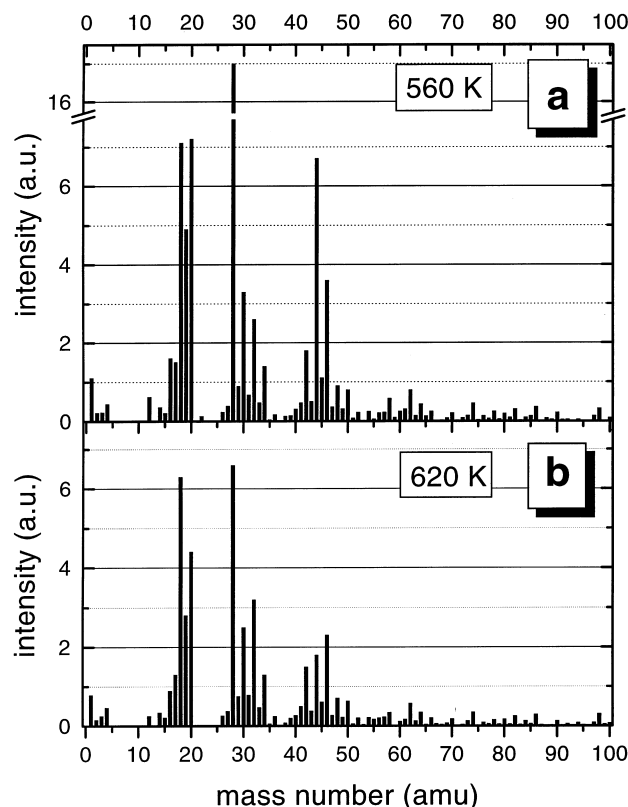


Fig. 7. Mass spectra of a soft a-C:D films (set A) recorded at (a) the temperature of maximum 28-amu-desorption in Fig. 6 (560 K) and at (b) 620 K (cf. dashed lines in Fig. 6). Given is the mean temperature of each spectrum. The total time for one mass scan is about 40 s corresponding to 12 K temperature increase during sampling of one spectrum. Please observe that the y axis in (a) is broken.

film density. Therefore we use in the following the film thickness as an indicator of the remaining amount of carbon.

The change of the thickness of the two sets of films investigated in this study is compared in Fig. 8. The film with the highest initial (D+H)/C ratio of about 1.3 (set B) is the most unstable one. Thermal decomposition in air starts already at 500 K. That is about 50 K lower than for the film with an initial (D+H)/C ratio of 0.96 (set A). The decomposition in vacuum was investigated for a-C:D:H films from set B. Decomposition starts at higher temperatures than in air, but these layers sublime completely, although no reactive atmosphere is present. The change of thickness for the hard a-C:D layers investigated in our previous work [12] is also shown in Fig. 8. The thermally-induced decomposition of these hard films with an initial D/C ratio of 0.4 starts in air at a temperature of 650 K and above, but the temperature necessary to completely remove the carbon layer is very similar to that of the soft films (725–750 K). It should be mentioned here that no measurable weight loss was found for pyrolytic graphite exposed to air up to temperatures of 800 K [23], which means that graphitic material is stable against oxidation at these temperatures. Therefore, we conclude that the dominant carbon release mechanism in the temperature range up to about 650 K is not the formation of volatile oxides. The question, what causes the observed loss of carbon in this range can be answered by the vacuum annealing and TDS experiments.

The most striking difference between soft and hard films is the behavior under annealing in vacuum (Fig. 8). While soft films evaporate completely in vacuum, hard films lose only about 5–10% of the total carbon (Fig. 2 in Ref. [12]) and annealing at higher temperature and/or extended annealing durations leads to the release of hydrogen and progressive graphitization of the remaining carbon layer [24]. The increase in thickness by about 12% of the hard a-C:D layer during annealing in vacuum shown in Fig. 8 is again attributed to a release of intrinsic mechanical stress. Together with the loss of about 5% of the carbon this causes a drop of the film density by about 15%. TDS investigations have shown that hard a-C:H layers loose hydrogen predominantly in form of H₂. Only about 10% are lost in form of hydrocarbons [14,22,25,26]. With increasing initial hydrogen content the fraction of released hydrocarbons increases and for soft films, like the ones investigated in this study, C_xD_y molecules dominate the released material [14,25]. This is in excellent agreement with the results presented in Figs. 6 and 7, although the caveat has to be added that the shown mass and TD spectra are not quantitative, because they are not corrected for the different sensitivity factors of the measured species. However, the dominance of C_xD_y species is obvious in these spectra. Furthermore, all C_xD_y species show a pronounced peak in the range from 550 to 620 K. This is also the temperature range where the dominant loss of carbon occurs for soft films (see Fig. 8). We therefore conclude that the dominantly released products in the temperature range

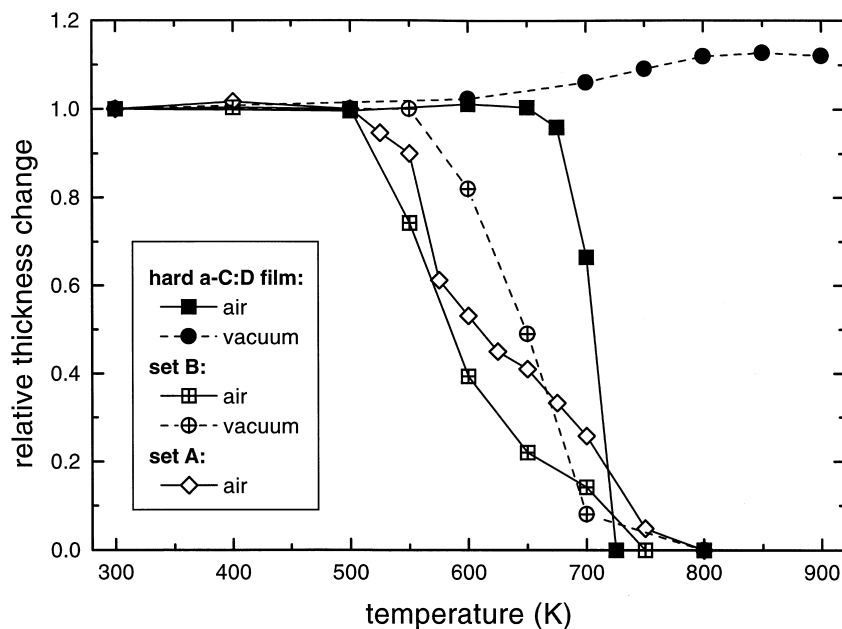


Fig. 8. Comparison of the thickness change of soft a-C:D films during annealing for 1 h in air and vacuum, respectively, for the samples shown in Figs. 1 and 5. In addition, data for hard a-C:D films from our preceding study [12] are also shown.

between 550 and 650 K are C_xD_y species. This release of hydrocarbons or hydrocarbon fragments does not require participation of other reactive species because it occurs in vacuum and probably also in air. The strongest signals observed are for CD_4 and C_2D_2 (Figs. 6 and 7). However, the dominant release of these compounds should be accompanied by a decrease of deuterium larger than that of carbon and the D/C ratio should decrease. Nevertheless, the composition of the remaining film does not change markedly up to 700 K. The two mass spectra presented in Fig. 7 show the release of many heavier hydrocarbon fragments which can be assigned to C_xD_y , with y being close to x , in part even smaller. Taking into account that the sensitivity of the mass analyzer decreases rapidly with increasing mass number and that the number of carbon atoms in one molecule increases with mass number, the observed product spectrum presented in Fig. 7 implies that a significant fraction of the released material consists of long chain C_xD_y fragments with x/y about 1 and is therefore in satisfactory agreement with the observation that during annealing in vacuum the D/C ratio of soft films remains almost unchanged.

The difference of the thickness decrease of the a-C:D:H films (set B) for vacuum and air may be due to a participation of oxygen or water from the ambient atmosphere in the decomposition process which causes a faster decomposition in air as compared with vacuum. However, we also find indirect hints that the released product spectrum differs in both cases. Fig. 5 shows that for annealing in vacuum the ratio of hydrogen to carbon in the remaining film stays almost constant up to 700 K when 90% of the total material is released. That means, that the average composition of the released species must have a similar (H+D)/C ratio of about 1.3 as the original film, which is, as discussed above, in satisfactory agreement with the results of the TDS measurements presented in Figs. 6 and 7. On the other hand, the abrupt decrease of the deuterium concentration for annealing in air above 550 K is not accompanied by an equivalent carbon removal (Figs. 1 and 3). Hence, in air the loss of hydrogen isotopes proceeds much faster than in vacuum. The quantitative IBA results further show that the loss of deuterium is accompanied by an increase of the total amount of hydrogen and oxygen in spite of a decrease in film thickness. This implies that the oxygen and hydrogen concentration in the remaining material increases considerably. This could be due to a replacement of deuterium by oxygen or OH groups. Infrared analysis has proven that oxygen is incorporated chemically in form of carbonyl and O–H groups (Fig. 4). The increase of the hydrogen content is, however, not accompanied by an increase of the C–H stretching vibrations. This implies that in this temperature range no efficient isotope exchange occurs and we conclude that hydrogen incorporation during annealing in air is due to

incorporation of O–H groups. Therefore, two processes remain to account for the rapid decrease of the deuterium content during annealing in air. The first is the release of C_xD_y hydrocarbons, most probably dominated by the release of terminal CD_3 groups, which was shown to be the rate determining step in the thermal decomposition of a-C:H films [26]. The release of C_xD_y hydrocarbons leads also to the observed decrease of the amount of carbon. The second processes is the displacement of deuterium by reactions of the material with oxygen and/or water from the ambient atmosphere. Deuterium may be lost as D_2 or through the formation of deuterated water, D_2O or HDO.

The fact that two different erosion mechanisms exist is evident from the time-dependent measurements presented in Fig. 3. At 550 K we observe a rapid decrease of the total carbon amount within the first 2 h and an even stronger decrease of the deuterium. Table 2 presents the corresponding quantitative ion-beam analysis results. The averaged D/C ratio of the released material in the first hour of annealing is about 2.5, decreasing to about 1 in the following hours. After 4 h of annealing the D/C ratio of the further released products drops even below 1. The averaged D/C ratio for the material released between 1 and 16 h of annealing in air is 0.78. These quantitative results are a strong indication that the released material changes as a function of annealing time. The data are in good accordance with the picture that in the initial phase C_xD_y hydrocarbons participate in the erosion process and in later phases volatile carbon oxides take over. The data in Fig. 3 show that a further loss of material is suppressed when most of the deuterium is released after about 8 h annealing. Similarly, at 650 K the carbon loss rate, which is initially a factor of 5 higher than at 550 K, decreases and the further erosion proceeds much slower after all deuterium is released. The change of film thickness for the soft a-C:D films (set A) at 550 and 650 K (Fig. 3) is compared with the thickness decrease of the hard a-C:D film of our previous study [12] in Fig. 9. It is obvious from Fig. 9 that the removal of soft films is much faster at 650 K than at 550 K. The initial removal rate of soft films is even notably higher at the much lower temperature of 550 K than that of hard films at 650 K, but after all deuterium is released (after 8 h in both cases) the removal of the hard film at 650 K proceeds faster than that of the soft film at 550 K. The removal rate of the soft film at 650 after complete release of the deuterium (after 30 min) is comparable to the rate for the hard film at 650 K when all deuterium is released.

As the removal of carbon atoms from soft films at temperatures up to 550 K is due to the release of hydrocarbon molecules, the erosion slows down as soon as most of the deuterium is lost. Although ion-beam and infrared analyses of the films exposed to air at 550 K show the incorporation of considerable amounts of

Table 2

Total amounts of remaining material and differential material loss for the samples annealed for various durations in air at a temperature of 550 K (cf. Fig. 3). (the differential loss is calculated from the additional material loss with respect to the previous annealing step)

Annealing duration (h)	Remaining material		Differential material loss		
	C (10^{15} cm^{-2})	D (10^{15} cm^{-2})	C (10^{15} cm^{-2})	D (10^{15} cm^{-2})	D/C ratio of lost material
0	1336	1142	–	–	–
1	1050	431	286	711	2.5
2	848	213	202	218	1.1
4	778	122	70	91	1.3
8	583	61	191	61	0.32
16	551	42	32	19	0.60
2–16	Average from 2 to 16 h		499	389	0.78

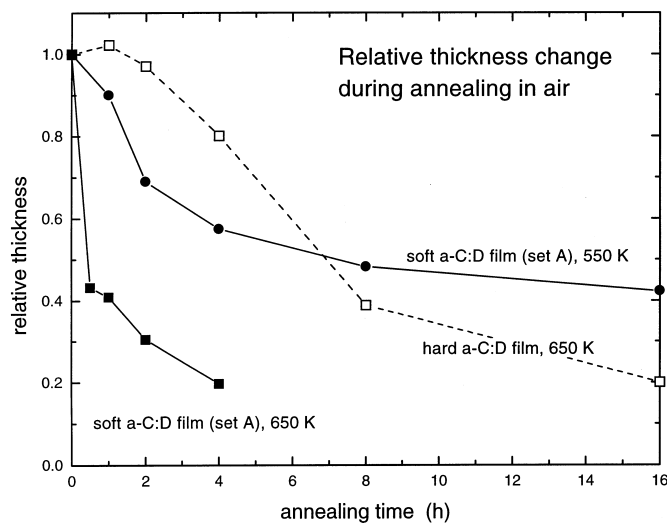


Fig. 9. Comparison of the thickness change of soft a-C:D films during annealing at a fixed temperature of 550 K (solid circles) and 650 K (solid squares), for the samples shown in Fig. 3. In addition, data for the annealing of a hard a-C:D film at 650 K (open squares) from our preceding study [12] are also shown.

oxygen chemically bonded to carbon, the temperature is obviously insufficient to cause a substantial erosion by thermal desorption of volatile oxides. This is evident from the time-dependent experiment shown in Fig. 3. For an efficient production of volatile carbon oxides temperatures above 650 K are necessary. Therefore, further loss of material is suppressed when all terminal C_xD_y groups are released.

We propose the following thermally-activated erosion scheme for the removal of soft amorphous hydrogenated layers during annealing in air.

- Up to temperatures of about 500–550 K structural changes occur in the films, but no significant loss of material is observed. The structural changes are due to the thermally-activated release of intrinsic stress

in the films and lead to a reduction of the density of the material.

- In the temperature range between 550 and 650 K C_xD_y hydrocarbons are released causing a pronounced loss of carbon and deuterium. The remaining mostly hydrogen-free carbon films are not efficiently removed by oxidation in this temperature range.
- At temperatures above 650 K oxidative removal of carbon through the formation of volatile oxides (CO and CO_2) starts leading to a complete removal of the layer.

This erosion scheme for soft films is very similar to that for the hard films beside the release of C_xD_y hydrocarbons in the range from 550 to 650 K which does not occur for hard films. From the comparison of the

release characteristics of the two types of soft films investigated in this work (sets A and B) we conclude that the amount of lost material in the intermediate temperature range (550–650 K) and accordingly the level of the plateau depends on the initial hydrogen isotope fraction of the layers. Set A with a initial hydrogen content of about 50% (D/C ratio 0.96) shows a clear plateau in this range (Fig. 1) and even after extended annealing durations at 550 K of up to 16 h more than 40% of the carbon is still present (Fig. 3). For the other set B with 58% hydrogen isotopes ((H + D)/C = 1.34) this plateau does not emerge or is considerably lower than for set A (Fig. 1, see also Fig. 8). Hard films with a hydrogen isotope fraction of 0.29 (D/C ratio of 0.4) do not at all decompose at these temperatures and more than 650 K are required to remove the films.

Haasz et al. [9] investigated the erosion of a-C:D layers in a pure oxygen atmosphere. The films were exposed in situ to oxygen at a temperature of 473 K and an initial oxygen pressure of 7 Torr (=9.3 Pa). The reaction products were monitored by mass spectrometry over a duration of 7 days. The films were initially about 220 nm thick and after 7 days exposure to oxygen about 35 nm have been removed. CO₂ and D₂O were found to be the main reaction products and 99% of the deuterium was released in the form of D₂O. Only 1% was found as D₂ and especially no methane was detected. These results seem at the first glance to be in contradiction to the erosion scheme suggested above. However, several reasons could account for the observed discrepancies. First, although a variety of surface analyses have been employed by Haasz et al. [9] the film stoichiometry was not determined unambiguously by quantitative methods, so that the film structure is not well known. From the D/C ratio estimated by Haasz et al. we infer that the film might be intermediate between soft and hard films. Second, the films were deposited at a wall temperature of 473 K and then exposed to oxygen at the same temperature. Therefore, the thermally-activated release of C_xD_y species cannot at all be anticipated. Third, the product spectrum measured by Haasz et al. does not necessarily represent the spectrum of the primary-released products, but the thermodynamical equilibrium gas composition of the system. The erosion process in the experiment of Haasz et al. proceeded much slower than in our experiment. Due to this low erosion rate and the extremely long residence time of the released products in the reaction chamber it is conceivable that the gas composition is merely determined by the establishment of the thermodynamic equilibrium gas composition. The low erosion rate at the relatively low temperature of 473 K is in accordance with our results showing that an efficient removal occurs only for temperatures higher than 500 K (Fig. 8). In agreement with our results from infrared analysis (Fig. 4), Haasz et al. detected the incorporation of oxygen and hydrogen in form of –OH, –

C=O, and –COOH complexes. According to the lower temperature and possibly a different film structure, the absolute amounts are, however, significantly lower.

5. Conclusion

In conclusion, the thermally-activated decomposition of soft amorphous deuterated carbon films (a-C:D) during annealing in air and vacuum was investigated using quantitative ion-beam analysis and profilometry and qualitative infrared and thermal desorption analyses. In both cases of annealing in air and in vacuum the films initially undergo minor structural modifications leading to a slight decrease in density. At temperatures above 500 K a pronounced reduction of the film thickness occurs and the thickness decreases proportional to the decrease of the areal density of carbon indicating only small changes in film density.

The loss of carbon in the range between 550 and 650 K is accompanied by a substantial decrease of the deuterium content and infrared analysis revealed the disappearance of all C–D related bands. After release of most of the deuterium the films show an increased resistivity against erosion by heat treatment because the remaining carbon rich film can no longer release volatile hydrocarbon molecules and the temperature is insufficient to release volatile oxides. At temperatures above 650 K the erosion of the films proceeds by the release of CO and CO₂ molecules similar to earlier results from hard a-C:D films [12].

When soft a-C:D films are annealed in vacuum all components including deuterium decrease proportionally to the decrease of film thickness. TDS revealed the evolution of many C_xD_y type hydrocarbons. In spite of the observed evolution of deuterium rich molecules such as CD₄, the composition of the remaining films did not change much from the initial CD_{1.0}. The evolution of high molecular weight fragments is considered to be responsible to maintain the original composition of the films after annealing in vacuum.

A scheme for the thermally-activated erosion of soft a-C:D layers was proposed. The key mechanisms leading to the erosion of soft a-C:D layers are the release of C_xD_y hydrocarbons beginning at 550 K and the formation of volatile oxides at temperatures above 650 K.

References

- [1] P. Koidl, C. Wild, R. Locher, R.H. Sah, in: R.E. Clausing, L.L. Horton, J.C. Angus, P. Koidl (Eds.), *Diamond and Diamond-Like Films and Coatings*, NATO-ASI Series B, vol. 266, Plenum, New York, 1991, p. 243.
- [2] A. von Keudell, W. Jacob, *Appl. Phys. Lett.* 66 (1995) 1322.

- [3] A. von Keudell, W. Jacob, *J. Appl. Phys.* 79 (1996) 1092.
- [4] A. von Keudell, W. Jacob, *J. Appl. Phys.* 81 (1997) 1531.
- [5] J. Winter, *J. Nucl. Mater.* 145–147 (1987) 131.
- [6] R.A. Causey, W.L. Christman, W.L. Hsu, R. Anderl, B. Wishard, *J. Vac. Sci. Technol. A* 7 (1989) 1078.
- [7] R.A. Causey, W.R. Wampler, D. Walsh, *J. Nucl. Mater.* 176&177 (1990) 987.
- [8] S. Chiu, A.A. Haasz, *J. Vac. Sci. Technol. A* 9 (1991) 747.
- [9] A.A. Haasz, S. Chiu, J.E. Pierre, Y.I. Gudimenko, *J. Vac. Sci. Technol. A* 14 (1996) 184.
- [10] G. Federici, R. Anderl, J.N. Brooks, R. Causey, J.P. Coad, D. Cowgill, R. Doerner, A.A. Haasz, G. Longhurst, S. Luckhardt, D. Mueller, A. Peacock, M. Pick, C.H. Skinner, W. Wampler, K. Wilson, C. Wong, C. Wu, D. Youchison, *Fus. Eng. Design*, in press.
- [11] G. Federici, P. Andrew, J.N. Brooks, R.A. Causey, J.P. Coad, R. Doerner, A.A. Haasz, G. Janeschitz, G.R. Longhurst, A. Peacock, V. Philipps, J. Roth, C.H. Skinner, and W.R. Wampler, in: *Proc. 13th Int. Conf. on Plasma–Surface Interactions in Controlled Fusion Devices (PSI 13)*, San Diego, CA, May 1998, *J. Nucl. Mater.* (1999) in press.
- [12] W. Wang, W. Jacob, J. Roth, *J. Nucl. Mater.* 245 (1997) 66.
- [13] A. Annen, R. Beckmann, W. Jacob, *J. Non-Cryst. Solids* 209 (1997) 240.
- [14] W. Jacob, R. Beckmann, F.-P. Bach, to be published.
- [15] R. Amirikas, D.J. Jamieson, S.P. Dooley, *Nucl. Instr. and Meth. B* 77 (1993) 110.
- [16] J.E.E. Baglin, A.J. Kellock, M.A. Crockett, A.H. Shih, *Nucl. Instr. and Meth. B* 64 (1992) 469.
- [17] F. Besenbacher, I. Stensgaard, P. Vase, *Nucl. Instr. and Meth. B* 15 (1986) 459.
- [18] A. von Keudell, W. Jacob, *J. Vac. Sci. Technol. A* 15 (1997) 402.
- [19] J. Biener, A. Schenk, B. Winter, J. Küppers, *J. Electron Spectr. Relat. Phenom.* 64&65 (1993) 331.
- [20] J. Biener, A. Schenk, B. Winter, C. Lutterloh, U.A. Schubert, J. Küppers, *Surf. Sci.* 307–309 (1994) 228.
- [21] H. Günzler, H.M. Heise, *IR-Spektroskopie: Eine Einführung*, 3rd edition, Verlag Chemie, Weinheim, 1996.
- [22] J. Biener, A. Schenk, B. Winter, C. Lutterloh, U.A. Schubert, J. Küppers, *Appl. Phys. Lett.* 61 (1992) 2414.
- [23] W. Ottenberger, W. Jacob, J. Roth, unpublished results.
- [24] M. Unger, W. Jacob, unpublished results.
- [25] P. Koidl, Ch. Wild, B. Dischler, J. Wagner, M. Ramsteiner, *Mater. Sci. Forum* 52&53 (1989) 41.
- [26] J. Küppers, *Surf. Sci. Rep.* 22 (1995) 249.